

Electron-phonon interaction contribution to the total energy of group IV semiconductor polymorphs: evaluation and implications

Arjun Varma R.,[†] Shilpa Paul,[†] Anup Itale,[†] Pranav Pable,[†] Radhika Tibrewala,[†] Samruddhi Dodal,[†] Harshal Yerunkar,[†] Saurav Bhaumik,[‡] Vaishali Shah,[¶] M. P. Gururajan,[†] and T. R. S. Prasanna^{*,†}

[†]*Department of Metallurgical Engineering and Materials Science, Indian Institute of Technology Bombay, Mumbai 400076, India*

[‡]*Department of Mathematics, Indian Institute of Technology Bombay, Mumbai 400076, India*

[¶]*Department of Scientific Computing, Modeling and Simulation, Savitribai Phule Pune University, Pune 411007, India*

E-mail: prasanna@iitb.ac.in

Abstract

In density functional theory (DFT) based total energy studies, the van der Waals (vdW) dispersion and zero-point vibrational energy (ZPVE) correction terms are included to obtain energy differences between polymorphs. We introduce a new correction term, due to electron-phonon interactions (EPI). We derive the expression for the EPI contribution to the total energy by extending Allen's general formalism to obtain the free energy contributions due to quasiparticle interactions. This expression is valid for all classes of materials - semiconductors, insulators and metals. Using this expression in combination with the Allen-Heine theory for the EPI corrections, we calculate EPI corrections to the total energy for cubic and hexagonal polytypes of Carbon, Silicon and Silicon Carbide. The EPI corrections alter the energy differences between polytypes in C, Si, and SiC; especially in C and SiC where the EPI strength is significant. In SiC polytypes, the EPI correction term is more sensitive to crystal structure than the vdW and ZPVE terms making it more important in determining energy differences. It clearly establishes that, in *ab initio* studies, the cubic SiC-3C is metastable and hexagonal SiC-4H is the stable polytype. Our results are consistent with the experimental results of Kleykamp. Our study enables the inclusion of EPI corrections as a separate term in the free energy expression. This opens the way to study their role on all thermodynamic properties through the Quasi-Harmonic Approximation.

Introduction

The group IV semiconductors, especially C, Si and SiC, are of immense scientific and technological importance. Currently, there is enormous interest in predicting new allotropes of C and Si because different crystal structures exhibit differing physical properties and provide a landscape to design materials with specific properties.¹⁻⁵ In the case of C, this is evident from the 522 allotropes listed in the Samara Carbon allotrope database.⁶ In Si, predicting metastable crystal structures with direct band-gaps are of particular interest.⁷ SiC polytypes

are among the most important materials for structural applications.⁸ SiC also has promising potential in future high-voltage and low-loss power devices.⁹

Given their importance, several studies have been performed on C, Si and SiC polymorphs. The accurate determination of the energy differences is essential in the study of these polymorphs. Despite several studies, the stable structure in SiC remains controversial in both experimental and computational studies because of the marginal energy differences between the cubic and hexagonal SiC polytypes. We first summarize the results from experimental studies and later from computational studies.

Greenberg et al.¹⁰ report thermodynamic data at 298 K for hexagonal α -SiC and cubic β -SiC using calorimetric studies. Using the quadrature rule for error propagation, the free energy of transformation can be calculated from their results to be $\Delta_{tr}G_{298}^{0,\alpha\rightarrow\beta} = -1.13 \pm 2.6$ kJ/mol and the enthalpy of transformation is $\Delta_{tr}H_{298}^{0,\alpha\rightarrow\beta} = -1.09 \pm 2.6$ kJ/mol. From the JANAF-Tables,^{11,12} the enthalpy of transformation is obtained as $\Delta_{tr}H_{298}^{0,\alpha\rightarrow\beta} = -1.7 \pm 8.9$ kJ/mol. From these results, we may conclude that the cubic β -SiC has lower enthalpy. However, the large margin of error suggests that the experimental results from calorimetric studies are not conclusive but are indicative.

In later studies, Kleykamp¹² reports the results of galvanic cell measurements and found that hexagonal α -SiC is stable. In this study, the stable structure was obtained directly from emf measurements in galvanic cells. In the temperature range of 1100 K - 1300 K, the cell arrangement with β -SiC in the negative electrode and α -SiC in the positive electrode gave a positive emf of 20 ± 5 mV (indicating a spontaneous process) leading to a Gibbs free energy of transformation $\Delta_{tr}G^{\beta\rightarrow\alpha} = -8 \pm 2$ kJ/mol. Unlike in most studies, in this study the stability of α -SiC is outside the margin of error. Kleykamp¹² reports that α -SiC is also stable at room temperature. For comparison, if the cubic β -SiC were the stable polytype, there would be no positive emf in the above cell arrangement. Because of the contrasting nature of the results in electrochemical studies, such experiments give clear indication of the stable polytype. This highlights the importance of Kleykamp's study.¹² A review of various

methods to obtain thermodynamic data for ceramic systems considers Kleykamp’s study as an elegant method to obtain small free energy differences and that this was the first time the free energy difference between the two SiC phases was directly measured.¹³

Due to these disagreements in the experimental results, a recent view is that there is no general agreement on the stable SiC polytype.¹⁴ However, based on the above discussion, it is clear that the available experimental data in favor of α -SiC as the stable polytype is much stronger. If the results of Kleykamp¹² are confirmed by independent electrochemical studies, they will clearly establish the stability of α -SiC under ambient conditions.

Computational studies using various DFT codes have consistently shown that the hexagonal SiC-6H and SiC-4H (α -SiC) are marginally stable compared to cubic SiC-3C (β -SiC) by a few meV/formula units (f.u.) or by < 1 kJ/mol.^{15–22} Kawanishi et al.¹⁷ and Scalise et al.¹⁸ included the vdW dispersion through the DFT-D2 approximation and found that SiC-3C is the stable polytype. However, Ramakers et al.²² have recently studied the stability using ten different vdW dispersion approximations including DFT-D2, DFT-D3, DFT-D3(BJ) and the advanced many-body dispersion (MBD) approximations. They conclude that dispersion approximations do not have any significant effect on the stability order of SiC polytypes compared to DFT studies. They conclude that SiC-3C is metastable at all temperatures after vibrational free energy contributions are included, similar to the results of Heine et al.^{19–21} We note that these results are consistent with the experimental results of Kleykamp¹² discussed above, though the energy differences between polytypes are much smaller in DFT studies.

Recently, for materials where polymorphs differ marginally in energy (SiC, BN, B, Fe₂P etc.), the stable polymorph has been determined by including the vdW dispersion and the zero-point vibrational energy (ZPVE) corrections. Including these corrections frequently alters the polymorph stability order.^{17,18,23–26}

However, these studies do not consider the contributions from electron-phonon interactions (EPI). Electron-phonon interactions have been well studied for their role in several

electronic and optical properties.^{27,28} In semiconductors and insulators, the experimental observation of the temperature dependence of band gaps is explained by the temperature dependence of eigenenergies, $E_{n\mathbf{k}}(T)$, due to EPI.^{27,28} Because all the eigenenergies are temperature dependent, $E_{n\mathbf{k}}(T)$, it follows that the total energy will also become temperature dependent when EPI contributions are included. Hence, the role of EPI in total energy and other thermodynamic properties must be studied.

In this paper, we introduce, for the first time, EPI corrections to the total energy and free energy. In order to do so, we first derive the expressions for the EPI contributions to the total energy by extending Allen’s general formalism developed to include contributions from quasiparticle interactions in the Quasi-Harmonic Approximation (QHA).²⁹ The expression for the EPI contribution to the total energy is general and valid for all classes of materials - semiconductors, insulators and metals. We provide supporting evidence from literature for this expression. We then show that, in semiconductors and insulators, the EPI contributions to the total energy and free energy can be obtained from the Allen-Heine theory. We use this approach to calculate the EPI correction to the total energy for C, Si and SiC polytypes.

Including the EPI corrections alters the energy differences between polytypes in C, Si and SiC. For SiC polytypes, the EPI term is more important, compared to the ZPVE and the vdW dispersion terms, in determining relative stability. Inclusion of the EPI term clearly establishes the metastability of the cubic SiC-3C polytype in *ab initio* studies. Our approach enables the inclusion of EPI corrections as a separate term in the free energy expression. This opens the way to study the role of EPI on all thermodynamic properties through the QHA.

EPI contributions to the free and total energy

Allen²⁹ has discussed the method for incorporating the renormalization of eigenenergies due to quasiparticle interactions (electron-phonon interactions, phonon-phonon interactions leading to anharmonicity) in the QHA. The procedure to include the contributions from

quasiparticle interactions is described in Sec-VI of Allen²⁹ titled “Corrections to the QH theory from QP renormalization”.

To calculate the EPI contributions, the starting point is Eq.1 of Allen²⁹ given by

$$\epsilon_K^{QP}(V, T) = \epsilon_K(V_0) + \Delta\epsilon_K^{QH} + \Delta\epsilon_K^{QP}(V, T) \quad (1)$$

where K represents (\mathbf{k}, n) , the wave-vector and band index respectively. The first term on the right-hand side is the eigenenergy for static lattice parameters. The second term is the change in eigenenergy when vibrational free energy is included to determine the equilibrium lattice parameters. The third term is the contribution from quasiparticle interactions (e.g. EPI). It is clear from Eq.3 of Allen’s paper²⁹ that the sum of the first two terms $(\epsilon_K(V_0) + \Delta\epsilon_K^{QH})$ is represented as $\epsilon_K(V)$.

When the third term in Eq. 1 is included, the eigenenergy is for interacting quasiparticles. As per Allen,²⁹ the free energy for non-interacting quasiparticles cannot be used when quasiparticle interactions are included. Hence, there are two different methods to calculate the free energy. For non-interacting quasiparticles, the free energy (method I) is given by Eq.11 of Allen.²⁹ For interacting quasiparticles, the free energy (method II) should be calculated from Eq.1 plus Eq.23 of Allen.²⁹ The difference in free energies calculated from these two methods, ΔF_{renorm} , is the contribution of quasiparticle interactions to the free energy. This is Allen’s formalism to include the contributions from quasiparticle interactions in QHA.

Allen²⁹ represents the EPI correction to the eigenenergy as $\Delta_{ep}\epsilon_K^{QP}$. From the structure of the symbol, it is clear that it is in the category of the third term in Eq. 1. Hence, we have to calculate the free energies from both methods described above and their difference is the EPI correction to the free energy, $\Delta F_{epi}(V, T)$.

We first calculate the free energy for non-interacting quasiparticles (from method I) where only the first two terms of Eq.1 ($= \epsilon_K(V)$) are to be used. In this case, the free energy is

obtained from Eq.11 of Allen's paper,²⁹ whose first, second and fourth lines are given as

$$\begin{aligned} F_{el}^{QH}(V, T) &= k_B T \sum_K \ln(1 - f_{K0}(V, T)) = \sum_K (\epsilon_K(V) - \mu(V)) + \Delta F_{el}^{QH}(V, T) \\ &\equiv E_{el}(V) + \Delta F_{el}^{QH}(V, T) \end{aligned} \quad (2)$$

where f_K is the Fermi-Dirac distribution given by

$$f_K = \frac{1}{\exp\left(\frac{(\epsilon_K(V) - \mu(V))}{k_B T}\right) + 1} \quad (3)$$

The equivalence in Eq. 2 has been justified on the grounds that $E_{el}(V)$ is more accurate than $(\sum_K (\epsilon_K(V) - \mu(V)))$ and must be used.²⁹

Eq. 2 is the standard expression used in QHA³⁰ for the electronic energy where non-interacting particles are assumed. The second term in Eq. 2, $\Delta F_{el}^{QH}(V, T)$ is due to the temperature dependent occupancies of electron eigenstates. Its contribution to the energy is given by³⁰

$$\Delta E_{el}^{QH}(V, T) = \int n(\epsilon) f \epsilon d\epsilon - \int_0^{\epsilon_F} n(\epsilon) \epsilon d\epsilon \quad (4)$$

Its contribution to the entropy is given by³⁰

$$\Delta S_{el}^{QH}(V, T) = -k_B \int n(\epsilon) [f \ln f + (1 - f) \ln(1 - f)] d\epsilon \quad (5)$$

For semiconductors and insulators, the occupied energy levels are well below the Fermi level, due to which $f \cong 1$ for all occupied levels and $\cong 0$ for unoccupied levels at all temperatures. Therefore, Eq. 2 becomes

$$F_{el}^{QH}(V, T) = k_B T \sum_K \ln(1 - f_{K0}(V, T)) = \sum_K (\epsilon_K(V) - \mu(V)) \equiv E_{el}(V) \quad (6)$$

We next calculate the free energy (from method II) for interacting quasiparticles, where the interaction is due to EPI. This is obtained from Eq.1 plus Eq.23 of Allen.²⁹ In this case,

all the three terms in Eq. 1 are present. Eq.23 of Allen²⁹ is given as

$$S_{el} = -k_B \sum_K [f_K \ln f_K + (1 - f_K) \ln(1 - f_K)] \quad (7)$$

For semiconductors and insulators, $f_K \approx 1$ and the entropy contribution in method II is ≈ 0 . Thus, the free energy contribution reduces to the contribution from the energy term. This is given by the summation over occupied states of all the three terms in Eq. 1.

$$F_{el}^{QH}(V, T) = \sum_K (\epsilon_K(V_0) + \Delta\epsilon_K^{QH} + \Delta_{ep}\epsilon_K^{QP}(V, T)) \quad (8)$$

From Eq.3 of Allen, the sum of the first two energy terms is $\epsilon_K(V)$ and the free energy can be written as

$$\begin{aligned} F_{el}^{QH}(V, T) &= \sum_K \epsilon_K(V) + \sum_K \Delta_{ep}\epsilon_K^{QP}(V, T) \\ &\equiv E_{el}(V) + \sum_K \Delta_{ep}\epsilon_K^{QP}(V, T) \end{aligned} \quad (9)$$

The equivalence in Eq. 9 follows from the justification given for the similar equivalence in Eq. 2 and Eq. 6.

The difference in the free energies from the two methods (Eq. 9 - Eq. 6) is the renormalization of the free energy, ΔF_{renorm} , due to EPI corrections. We refer to ΔF_{renorm} as $\Delta F_{epi}(V, T)$ which is given by

$$\Delta F_{epi}(V, T) = \sum_K \Delta_{ep}\epsilon_K^{QP}(V, T) = 2 \sum_{n, \mathbf{k}}^{occ, IBZ} w_{\mathbf{k}} \Delta\epsilon_{n\mathbf{k}}(V, T) \quad (10)$$

For semiconductors and insulators, the entropy contribution is ≈ 0 and the EPI contribution to the free energy is also the EPI contribution to the total energy and both are equal to the EPI contribution to the band-structure energy. Thus, the EPI contribution to the total energy is given by

$$\Delta E_{av}^{ep}(V, T) = \sum_K \Delta_{ep} \epsilon_K^{QP}(V, T) = 2 \sum_{n, \mathbf{k}}^{occ, IBZ} w_{\mathbf{k}} \Delta \epsilon_{n\mathbf{k}}(V, T) \quad (11)$$

The above formalism, when applied to metals, results in additional terms in the free energy (in both the methods I and II) that are not present in semiconductors and insulators. These are as follows: In method I, the second term in Eq. 2 ($\Delta F_{el}^{QH}(V, T)$) is non-zero and in method II, the entropy contribution is non-zero.

Regarding the EPI contribution to the total energy in metals, there are additional contributions due to the temperature dependent occupancies determined by the Fermi-Dirac distribution. However, because this contribution is present in both methods, the difference is likely to make a minor contribution to the EPI correction. In contrast, the third term ($\Delta_{ep} \epsilon_K^{QP}$) is present only in method II. Therefore, when the difference between the two methods is considered, the main contribution is from the inclusion of the third term $\Delta_{ep} \epsilon_K^{QP}(V, T)$ in method II. For total energy contribution, this term must be summed (or integrated) over occupied states. Thus, the EPI contribution to the band-structure energy is the main term in the EPI contribution to the total energy in metals. That is, Eq. 11 is the main term in the EPI correction to the total energy in metals as well.

Thus, Eq. 11 - the EPI contribution to the total energy is the EPI contribution to the band-structure energy - is a result of general validity and is applicable for all classes of materials - metals, semiconductors and insulators. Further, because it does not depend on the method of calculation, it is applicable to results from all EPI calculation methods such as Allen-Heine theory, *ab initio* molecular dynamics (AIMD) and other methods.

We note that in the literature, there is supporting evidence for Eq. 11. In some metallic systems, Mo,³¹ Zr,³² FeTi,³³ AIMD studies show that the electronic density of states (EDOS) is temperature dependent and at high temperatures the sharp features of the EDOS are smoothed. This has been attributed to adiabatic EPI.³³ It is clear that in such systems, EPI causes the EDOS and hence, the band-structure energy to be temperature dependent.

From Eq. 11, it follows that this temperature dependent band-structure energy is equal to and hence, should be the main cause for the temperature dependence of the total energy.

Asker et al.³¹ have used AIMD to determine the temperature dependent energy differences between bcc and fcc Mo. Static lattice calculations show that the energy difference between bcc and fcc Mo structures is 400 meV/atom at 0 K. At high temperatures (~ 3000 K), using AIMD, they obtain a configuration energy difference of 190 meV/atom. Under vibrating lattice conditions, the sharp features of the EDOS that are present for static lattice conditions are smoothed. This smoothing is specifically attributed by Asker et al.³¹ to be the main reason for the sharp change in the total energy at finite temperatures.

It is clear that in the above study, adiabatic EPI causes the EDOS (and hence, the band structure energy) to be temperature dependent and this in turn causes the total energy to be temperature dependent. This is entirely consistent with Eq. 11 and thus, the study of Asker et al.³¹ provides supporting evidence for it. Indeed, Eq. 11 should be considered to be the theoretical basis for the computational results.

EPI corrections to the total energy from the Allen-Heine theory

For semiconductors and insulators, the Allen-Heine theory³⁴⁻³⁸ is widely used to obtain the EPI corrections to the eigenenergies. In the Allen-Heine theory,³⁴⁻³⁸ electron-phonon interactions lead to contributions from the Fan-Migdal (FM)^{39,40} and the Debye-Waller (DW)⁴¹ terms to the eigenenergies. The temperature dependent eigenenergies are given by $E_{n\mathbf{k}}(T) = \epsilon_{n\mathbf{k}} + \Delta\epsilon_{n\mathbf{k}}(T)$ where $\epsilon_{n\mathbf{k}}$ is the static lattice eigenenergy for wave vector \mathbf{k} and band n and the EPI correction is given by $\Delta\epsilon_{n\mathbf{k}}(T) = \Delta^{FM}\epsilon_{n\mathbf{k}}(T) + \Delta^{DW}\epsilon_{n\mathbf{k}}(T)$. Due to the presence of zero-point vibrations, the zero-point renormalization (ZPR) of electron eigenenergies, $\Delta\epsilon_{n\mathbf{k}}(0)$, has finite values.

The Allen-Heine theory allows the calculation of EPI correction to any arbitrary eigen-

state, $\Delta\epsilon_{n\mathbf{k}}(T)$, including for the valence band maxima (VBM) and the conduction band minima (CBM). For this reason, it is the most widely used *ab initio* method in EPI studies of band gaps and band structures.⁴²⁻⁵⁴

Thus, we can also obtain the EPI correction to the \mathbf{k} -points in the irreducible Brillouin zone (IBZ) that contribute to the DFT total energy. This allows the EPI corrections to the band-structure energy and hence, from Eq. 11, the EPI contribution to the total energy to be calculated.

This is a simple method to calculate the EPI contributions to the total energy and free energy in semiconductors and insulators. Using this method, in this study, we calculate the EPI corrections to the total energy for the cubic and hexagonal polytypes of C, Si and SiC.

Computational Details

All calculations were performed using the ABINIT software package⁵⁵⁻⁵⁷ that has been used in several ZPR band-gap studies.^{45,50-54}

For SiC polytypes, the dispersion corrections (DFT-D2 and DFT-D3(BJ))^{58,59} were also applied to calculate the total energies and lattice parameters. DFT-Dn methods were chosen because of the advantage that the dispersion and EPI corrections are both incorporated by calculating the EPI corrections at the altered lattice parameters.^{52,60}

We present results obtained for the ONCV pseudopotentials with PBE exchange-correlation functional. Similar results were obtained for other pseudopotentials. (See Supplementary Information). The energy cutoffs used were 30 Ha (Si) and 50 Ha (C and SiC). For hexagonal structures, the Broyden-Fletcher-Goldfarb-Shanno (BFGS) algorithm was used for structural optimization.^{55,56} An unshifted $8 \times 8 \times 8$ \mathbf{k} -point grid was used for cubic structures. For all hexagonal structures (except for SiC-4H for which $9 \times 9 \times 3$ \mathbf{k} -point grid was used), an unshifted $9 \times 9 \times 5$ \mathbf{k} -point grid was used.

The module on temperature dependence of the electronic structure that calculates EPI

corrections using Allen-Heine theory was used.⁵⁷ We provide the list of \mathbf{k} -points in the IBZ and additional \mathbf{k} -points corresponding to CBM. The \mathbf{q} -point grids were increased by 200-300 \mathbf{q} -points in IBZ. To accelerate convergence, an imaginary smearing parameter, $i\delta$, of 100 meV and 50 meV were used.^{46,52,57} The optimized number of bands used was 30 for SiC-4H and 22 for all other C, Si and SiC polytypes. EPI corrections for SiC-6H could not be calculated due to computational constraints.

For IR-active materials, the non-adiabatic approximation must be used.⁴⁶ In this case, the ZPR shift, $\Delta\epsilon_{nk}(T)$, varies linearly with $1/N_q$, where N_q^3 is the total number of \mathbf{q} -points in the BZ.^{46,53} It follows from the linearity property of Eq. 11 that $\Delta E_{av}^{eq}(T)$ will also vary linearly with $1/N_q$ (Proof in Supplementary Information).

Results and Discussion

EPI contributions in carbon and silicon polytypes

Table 1 gives the lattice parameters, band gaps and the relative energy stability with and without EPI corrections for the C and Si polytypes. Our DFT lattice parameters and relative energies are similar to those in literature.^{2,61,62}

For C-dia, the ZPR of VBM, CBM and the lowest CB at Γ -point are 142 meV, -151.4 meV and -272.5 meV respectively. For Si-dia they are 34.27 meV, -21.24 meV and -8 meV respectively. These values are similar to the reported values.⁵⁷ Because, the ZPR for other eigenstates in the IBZ were obtained in the same run, it follows that they are reliable.

Figure 1 shows the convergence behavior of the EPI correction to the total energy, $\Delta E_{av}^{ep}(0)$, with $1/N_q$ for $i\delta = 100$ meV. A strong EPI correction is seen for carbon polytypes whereas a weak EPI correction is seen for silicon polytypes. This is consistent with the weaker electron-phonon interaction in silicon compared to carbon.⁴³⁻⁵² Figure 1 also shows a significant crystal structure dependence of the EPI correction to the total energy, especially

Table 1: The lattice parameters, band gaps and energy differences for carbon and silicon polytypes.

Material	a,c (Bohr)	Band gaps		ΔE (DFT) (meV/atom)	ΔE (DFT+EPI) (meV/atom)
		Indirect (eV)	Direct (eV)		
C-dia	6.75	4.18	5.61	0	0
C-hex	4.75, 7.90	3.40	5.01	24.3	67.9
Si-dia	10.34	0.61	2.55	0	0
Si-hex	7.28, 12.03	0.45	0.98	9.7	17.3

in carbon polytypes where the electron-phonon interaction is strong.

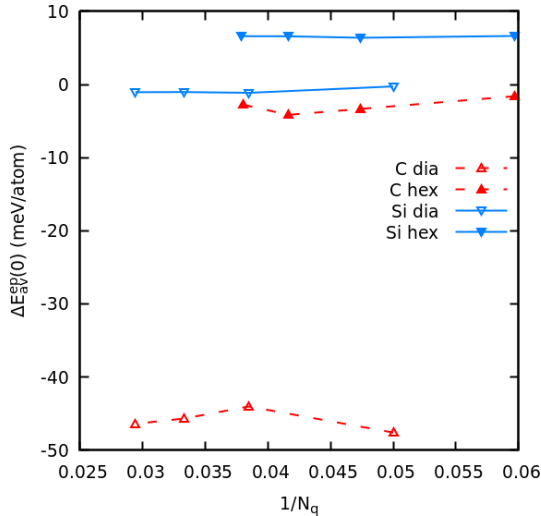


Figure 1: Convergence of EPI correction to total energy with \mathbf{q} -point grid density (adiabatic approximation) for a smearing parameter of 100 meV for Carbon and Silicon polytypes.

The negative value of $\Delta E_{av}^{ep}(0)$ for C-dia implies that, averaged over the BZ, the FM term is greater than the DW term. In contrast to C-dia, a small value of $\Delta E_{av}^{ep}(0)$ is obtained for C-hex. However, the ZPR of VBM, CBM and the lowest CB at Γ -point for C-hex are 117 meV, -172.6 meV and -313.9 meV respectively. They are comparable to those for C-dia indicating a strong electron-phonon interaction in C-hex. Thus, the small value of $\Delta E_{av}^{ep}(0)$ in C-hex indicates a near balance between the FM and DW terms when averaged over the BZ.

Table 1 shows that after including EPI corrections the C-dia structure is more stable

than the C-hex structure by ≈ 68 meV/atom compared to ≈ 24 meV/atom from DFT studies.^{2,61,62} The Si-dia stability also increases from ≈ 10 meV/atom to ≈ 17 meV/atom. It clearly follows that including EPI corrections in *ab initio* studies of relative stability of polymorphs is essential.

EPI contributions in SiC polytypes

Table 2 shows the lattice parameters, ZPR of the VBM/CBM and the energy stabilities relative to the SiC-3C polytype. The indirect/direct band gaps (at the Γ -point) are 1.41 eV/6.13 eV (SiC-3C), 2.32 eV/4.72 eV (SiC-2H), 2.26 eV/5.01 eV (SiC-4H) and 2.07 eV/5.10 eV (SiC-6H). These results are very similar to literature values.¹⁵⁻¹⁸

Table 2: Lattice parameters, ZPR and energy stability of SiC polytypes relative to SiC-3C for DFT, DFT-D2 and DFT-D3(BJ) calculations.

Polytype	a, c (Bohr)	ZPR VBM/CBM (meV)	ΔE (meV/f.u.)
3C-SiC			
DFT	8.28	93.6/-56.3	0
DFT-D2	8.23	-	0
DFT-3(BJ)	8.21	95.4/-55.6	0
4H-SiC			
DFT	5.85, 19.14	84.7/-61.3	-2.15
DFT-D2	5.81, 19.06	-	2.31
DFT-D3(BJ)	5.80, 18.99	86.3/-60.8	-1.81
2H-SiC			
DFT	5.84, 9.59	78.6/-88.9	5.07
DFT-D2	5.81, 9.56	-	14.2
DFT-D3(BJ)	5.80, 9.52	80.0/-86.5	6.32

In our DFT results, SiC-4H is more stable than SiC-3C, similar to previous studies.¹⁵⁻¹⁸ Including the DFT-D2 approximation makes SiC-3C to be the stable polytype, similar to recent studies.^{17,18} However, including the DFT-D3(BJ) approximation retains the DFT stability order where SiC-3C is metastable, consistent with the results of Ramakers et al.²² As discussed earlier, Ramakers et al.²² have considered ten different dispersion approximations

and concluded that the DFT stability order should be retained.

In Table 2, the ZPR of VBM/CBM for SiC-3C (obtained using parameters similar to those used in other studies⁵²) is comparable to reported values.⁵⁴

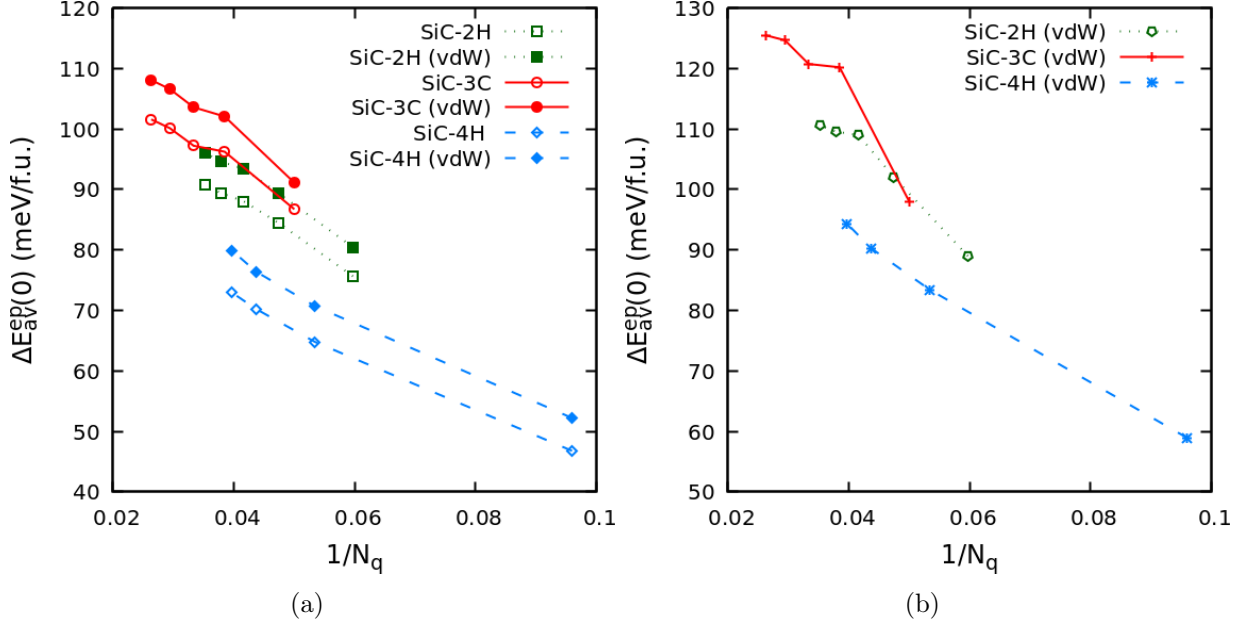


Figure 2: Convergence of EPI correction to total energy with \mathbf{q} -point grid density (non-adiabatic approximation) for smearing parameters: a) 100 meV and b) 50 meV, for SiC polytypes for DFT and DFT-D3(BJ) lattice parameters.

Figure 2 shows the convergence behavior of the EPI correction to the total energy, $\Delta E_{av}^{ep}(0)$. The $\Delta E_{av}^{ep}(0)$ for SiC-4H (50% hexagonality)^{17,18} does not lie between the values for SiC-3C (0% hexagonality) and SiC-2H (100% hexagonality). A similar trend is also seen for DFT total energies (Table 2 and Ref.^{15–18}).

Figure 2 shows that $\Delta E_{av}^{ep}(0)$ has a strong crystal structure dependence. For example, the EPI contribution to the total energy for SiC-3C and SiC-4H differ by > 20 meV/f.u. This difference is much higher than the marginal (1-2 meV/f.u.) difference in the DFT total energy.

Table 3 shows the stability of SiC-polytypes obtained by combining the EPI corrections to total energy in Figure 2 with the relative stability data in Table 2. For SiC-3C and SiC-

2H we consider $\Delta E_{av}^{ep}(0)$ for the smallest value of $1/N_q$. However, for SiC-4H, the $\Delta E_{av}^{ep}(0)$ varies by $\lesssim 3$ meV/f.u. for the smallest two $1/N_q$ values. Therefore, we report two values for SiC-4H in Table 3; the difference in $\Delta E_{av}^{ep}(0)$ a) between the smallest values of $1/N_q$ for SiC-3C and SiC-4H and b) at approximately the same $1/N_q \approx 0.039$. The actual stability value for SiC-4H is likely to be between these values.

Table 3: Relative stability (meV/f.u.) of SiC polytypes. In column-3, the second value corresponds to $1/N_q \approx 0.039$. The D2 values are estimated from DFT and D3(BJ) values as its lattice parameters are in-between their lattice parameters.

Polytype→ Stability ↓	SiC-3C	SiC-4H	SiC-2H
DFT + EPI (100meV)	0	-30.8/-25.5	-5.7
DFT-D2+ EPI(100 meV)	0	-25.6/-19.9	+2.8
DFT-D3(BJ)+ EPI (100meV)	0	-30.0/-24.0	-5.6
DFT-D3(BJ) + EPI (50meV)	0	-32.9/-27.6	-8.5

Table 3 shows the importance of EPI corrections. SiC-4H is the stable polytype with much greater relative stability (≥ 20 meV/f.u), irrespective of the DFT-D approximation, compared to the marginal stability (≈ 2 meV/f.u.) under DFT and DFT+vdW conditions. For SiC-2H, the relative stability depends on the DFT-D approximation used, though it is more stable in the widely used D3(BJ) approximation.^{23,63} However, the stability is < 10 meV/f.u., indicating that it is within the range of dispersion approximation errors.²³

The similar trends for $i\delta = 50$ meV suggests that SiC-4H will likely be the stable polytype when $i\delta$ is decreased further for full convergence.⁴⁶

With our results, we can assess the importance of the three correction terms to the DFT relative stability order of SiC polytypes. The ZPVE is relatively insensitive to crystal struc-

ture¹⁸ which is also reflected in the similar Debye temperatures of SiC polytypes.^{64,65} The D3(BJ) correction is also relatively insensitive to crystal structure. Both these terms contribute $\sim 1\text{-}2$ meV/f.u. each to the energy differences between SiC polytypes. In contrast, EPI correction contributes ≥ 22 meV/f.u to the energy differences (Figure 2) indicating much greater sensitivity to crystal structure. Clearly, the EPI term is the most important of the three correction terms to affect the relative stability of SiC polytypes. Hence, EPI contributions must be included in all studies of materials with polymorphs that differ marginally in energy where currently only ZPVE and vdW contributions are included.

After including vdW and EPI corrections to DFT, the relative stability order is SiC-4H, SiC-2H and SiC-3C. (As mentioned above, ZPVE contributed only $\sim 1\text{-}2$ meV/f.u. to energy differences.) The hexagonal SiC-4H is stable over the cubic SiC-3C by ~ 25 meV/f.u. or ~ 2.5 kJ/mol. Hence, by including EPI corrections, the stability of SiC-4H is significantly enhanced when compared to DFT studies, with or without the dispersion approximation. Our results are consistent with the experimental results of Kleykamp.¹² Our results also provide additional motivation to confirm (or contradict) Kleykamp's¹² results by independent electrochemical experimental studies. As discussed earlier, electrochemical studies can provide a clear and unambiguous indication of the stable SiC polytype.

We can also calculate the EPI corrections at finite temperatures. Figure 3 shows that at higher temperatures. $\Delta\epsilon_{vbm}(T)$ varies linearly with temperature, as predicted for all eigenstates.³⁸ The slope is $\lesssim 0.2$ meV/K similar to predicted values.^{34,38} In particular, the experimentally obtained slope for SiC-6H is 0.24 meV/K.⁶⁶ Our values are acceptable as the calculated values are known to be smaller than the experimental values of the slope (for bandgaps) in other materials.⁴⁶

It follows that the weighted sum, $\Delta E_{av}^{eq}(T)$, will also vary linearly with temperature and is seen in Figure 3. We note that $\Delta\epsilon_{n\mathbf{k}}(T)$ has both positive and negative values. For this reason, despite $8 e^-$ /f.u., the temperature variation of weighted sum, $\Delta E_{av}^{ep}(T)$, is only slightly larger, and not ≈ 8 times larger, than that for $\Delta\epsilon_{vbm}(T)$.

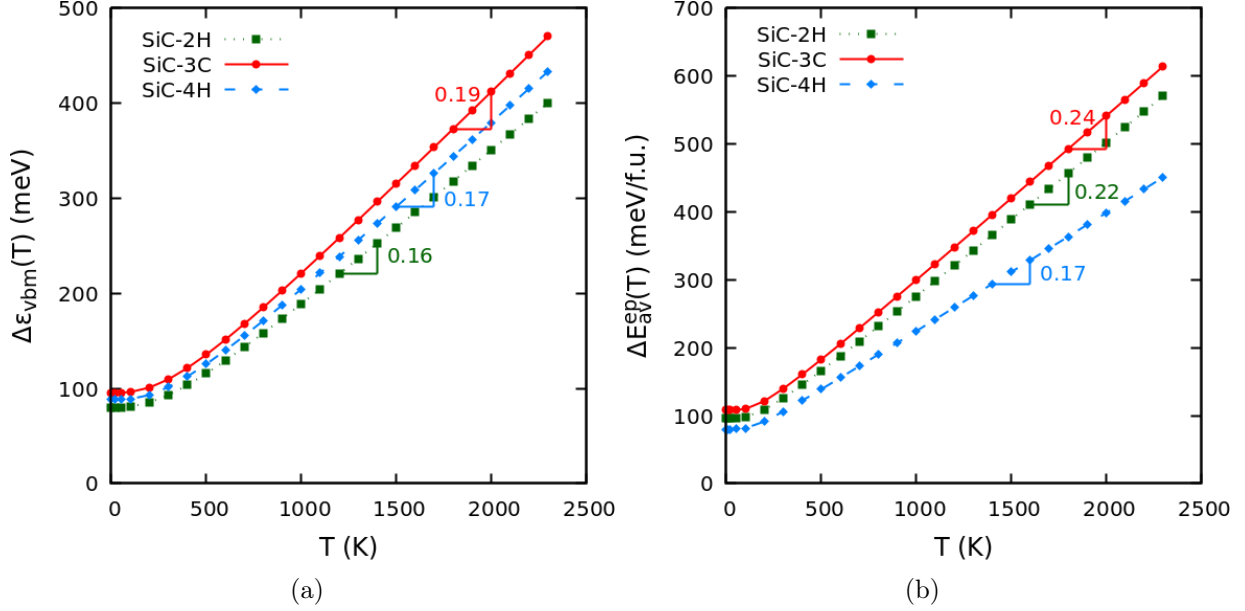


Figure 3: Finite temperature EPI corrections to (a) VBM and (b) total energy of SiC for DFT-D3(BJ) lattice parameters.

The thermodynamic properties are obtained from QHA where the Helmholtz free energy is given by^{67,68}

$$F(V, T) = E_0(V) + F_{vib}(V, T) + F_{elec}(V, T) \quad (12)$$

where $E_0(V)$ is the DFT total energy, $F_{vib}(V, T)$ is the vibrational free energy contribution and $F_{elec}(V, T)$ is the electronic contribution. Because the EPI contribution (Eq. 11) is now represented separately, it can be added in Eq. (S4) above.

Even after the EPI corrections are included, because the band gaps are of order eV, the electronic specific heat is ≈ 0 , consistent with experiments.⁶⁹ Theoretically, the EPI contribution to specific heat is negligible because the product $[f(\epsilon)(1 - f(\epsilon))] \approx 0$.³⁶ In QHA, from Eq. (S4), the EPI contribution to specific heat is obtained as $\Delta C_v^{ep}/T = -F_{epi}''(T) = -\Delta E_{av}''^{ep}(T)$. From Figure 3, at low temperatures, $\Delta E_{av}^{ep}(T)$ is constant and at high temperatures its first derivative is constant. Therefore, $\Delta C_v^{ep}(T) \approx 0$ at low and high temperatures, consistent with theory and experiments. In a small intermediate temperature range, an error is given that is unavoidable as $\Delta E_{av}^{ep}(V, T)$ changes from constant value to linear dependence

on temperature, leading to finite second derivative. In Figure 3, in the intermediate temperature range (100 K - 500 K), we estimate $-\Delta C_v^{ep}$ at 200 K to be $\approx 0.13, 0.12$ and 0.09 meV/K.f.u which drops rapidly at 300 K to $0.07, 0.06$ and 0.03 meV/K.f.u for SiC-3C, SiC-2H and SiC-4H respectively. The magnitudes are comparable to the vibrational specific heat at 200 K and are much less at 300 K.⁷⁰ Thus, because the errors are limited to a small temperature range, the role of EPI can be incorporated in QHA through $\Delta E_{av}^{ep}(V, T)$.

The differences in the thermodynamic properties (lattice parameters (and those dependent on them), thermal expansion, etc.) evaluated from Eq. (S4) with and without $\Delta E_{av}^{ep}(V, T)$ are the EPI contribution to the properties. The former is more appropriate for comparison with experimental values which include EPI contributions.

Our results have wide applicability. A significant EPI results in ZPR of VBM and other eigenstates in hundreds of meV in several materials.⁴²⁻⁵⁴ It also leads to strong crystal structure dependence of the ZPR(VBM) with its differences in tens of meV in AlN, BN and GaN polytypes.^{46,52,54} Because the ZPR(VBM) contributes to $\Delta E_{av}^{ep}(0)$, it follows that differences in $\Delta E_{av}^{ep}(0)$ between polymorphs of order of tens of meV/f.u. is a distinct possibility that must be evaluated. Our results for C and SiC polytypes support this suggestion.

Conclusion

We introduce a new correction term due to electron-phonon interactions to the DFT total energy. The expression for the EPI contribution to the total energy is derived by extending Allen's general formalism to obtain the free energy contribution due to quasiparticle interactions. This expression is valid for all classes of materials - semiconductors, insulators and metals. Using this expression in combination with the Allen-Heine theory for the EPI calculations, we calculate the EPI corrections to the total energy for C, Si and SiC polytypes. The EPI corrections alter the energy differences between polytypes in C, Si and SiC; especially in C and SiC where the EPI strength is significant. Compared to the ZPVE and vdW correc-

tion, the EPI correction term is more important in determining the relative stability order of SiC polytypes due to its greater sensitivity to crystal structure. It clearly establishes that in *ab initio* studies SiC-3C is metastable and SiC-4H is the stable polytype by significantly enhancing the energy differences. Our results are consistent with the experimental results of Kleykamp. Our study enables, for semiconductors and insulators, the inclusion of EPI corrections as a separate term in the free energy in QHA. This opens the way to study their role on all thermodynamic properties.

Acknowledgement

The authors thank the “Spacetime” HPC facilities at IIT Bombay for computational support.

References

- (1) Takagi, M.; Taketsugu, T.; Kino, H.; Tateyama, Y.; Terakura, K.; Maeda, S. Global search for low-lying crystal structures using the artificial force induced reaction method: A case study on carbon. *Physical Review B* **2017**, *95*, 184110.
- (2) Mujica, A.; Pickard, C. J.; Needs, R. J. Low-energy tetrahedral polymorphs of carbon, silicon, and germanium. *Physical Review B* **2015**, *91*, 214104.
- (3) He, C.; Shi, X.; Clark, S. J.; Li, J.; Pickard, C. J.; Ouyang, T.; Zhang, C.; Tang, C.; Zhong, J. Complex low energy tetrahedral polymorphs of group IV elements from first principles. *Physical Review Letters* **2018**, *121*, 175701.
- (4) Dmitrienko, V. E.; Chizhikov, V. A. Infinite family of bc8-like metastable phases in silicon. *Physical Review B* **2020**, *101*, 245203.
- (5) Haberl, B.; Strobel, T. A.; Bradby, J. E. Pathways to exotic metastable silicon allotropes. *Applied Physics Reviews* **2016**, *3*, 040808.

- (6) Proserpio, D. M. Samara Carbon Allotrope Database. <http://sacada.sctms.ru>, accessed July 15, 2021.
- (7) Lee, I.-H.; Lee, J.; Oh, Y. J.; Kim, S.; Chang, K.-J. Computational search for direct band gap silicon crystals. *Physical Review B* **2014**, *90*, 115209.
- (8) Riley, F. *Structural Ceramics*; Cambridge, UK: Cambridge University Press, 2009.
- (9) Kimoto, T. Material science and device physics in SiC technology for high-voltage power devices. *Japanese Journal of Applied Physics* **2015**, *54*, 040103.
- (10) Greenberg, E.; Natke, C. A.; Hubbard, W. N. The enthalpy of formation of silicon carbide by fluorine bomb calorimetry. *The Journal of Chemical Thermodynamics* **1970**, *2*, 193–201.
- (11) Chase Jr, M. W. JANAF thermochemical table. *J. Phys. Chem. Ref. Data* **1985**, *14*, Supplement–No.1, 633–634.
- (12) Kleykamp, H. Gibbs energy of formation of SiC: A contribution to the thermodynamic stability of the modifications. *Berichte der Bunsengesellschaft für physikalische Chemie* **1998**, *102*, 1231–1234.
- (13) Jacobson, N.; Putnam, R.; Navrotsky, A. In *Measurement of the Thermodynamic Properties of Multiple Phases*; Weir, R., De Loos, T., Eds.; Experimental Thermodynamics; Elsevier, 2005; Vol. 7; pp 307–325.
- (14) Drüe, M.; Kozlov, A.; Seyring, M.; Song, X.; Schmid-Fetzer, R.; Rettenmayr, M. Phase formation in the ternary system Li–Si–C. *Journal of Alloys and Compounds* **2015**, *653*, 474–479.
- (15) Park, C. H.; Cheong, B.-H.; Lee, K.-H.; Chang, K.-J. Structural and electronic properties of cubic, 2H, 4H, and 6H SiC. *Physical Review B* **1994**, *49*, 4485.

- (16) Käckell, P.; Wenzien, B.; Bechstedt, F. Electronic properties of cubic and hexagonal SiC polytypes from ab initio calculations. *Physical Review B* **1994**, *50*, 10761.
- (17) Kawanishi, S.; Mizoguchi, T. Effect of van der Waals interactions on the stability of SiC polytypes. *Journal of Applied Physics* **2016**, *119*, 175101.
- (18) Scalise, E.; Marzegalli, A.; Montalenti, F.; Miglio, L. Temperature-Dependent Stability of Polytypes and Stacking Faults in Si C: Reconciling Theory and Experiments. *Physical Review Applied* **2019**, *12*, 021002.
- (19) Heine, V.; Cheng, C.; Needs, R. J. The preference of silicon carbide for growth in the metastable cubic form. *Journal of the American Ceramic Society* **1991**, *74*, 2630–2633.
- (20) Rutter, M. J.; Heine, V. Energetics of stacking boundaries on the {0001} surfaces of silicon carbide. *Journal of Physics: Condensed Matter* **1997**, *9*, 8213.
- (21) Heine, V.; Cheng, C.; Needs, R. A computational study into the origin of SiC polytypes. *Materials Science and Engineering: B* **1992**, *11*, 55–60.
- (22) Ramakers, S.; Maruszyk, A.; Amsler, M.; Eckl, T.; Mrovec, M.; Hammerschmidt, T.; Drautz, R. Effects of thermal, elastic and surface properties on the stability of SiC polytypes. 2022; <https://arxiv.org/abs/2201.05379>.
- (23) Cazorla, C.; Gould, T. Polymorphism of bulk boron nitride. *Science Advances* **2019**, *5*, eaau5832.
- (24) Nikaido, Y.; Ichibha, T.; Hongo, K.; Reboredo, F. A.; Kumar, K. C. H.; Mahadevan, P.; Maezono, R.; Nakano, K. Diffusion Monte Carlo Study on Relative Stabilities of Boron Nitride Polymorphs. *The Journal of Physical Chemistry C* **2022**, *126*, 6000–6007.
- (25) van Setten, M. J.; Uijtewaal, M. A.; de Wijs, G. A.; de Groot, R. A. Thermodynamic stability of boron: The role of defects and zero point motion. *Journal of the American Chemical Society* **2007**, *129*, 2458–2465.

- (26) Bhat, S. S.; Gupta, K.; Bhattacharjee, S.; Lee, S.-C. Role of zero-point effects in stabilizing the ground state structure of bulk Fe₂P. *Journal of Physics: Condensed Matter* **2018**, *30*, 215401.
- (27) Giustino, F. Electron-phonon interactions from first principles. *Reviews of Modern Physics* **2017**, *89*, 015003.
- (28) Poncé, S.; Antonius, G.; Gillet, Y.; Boulanger, P.; Janssen, J. L.; Marini, A.; Côté, M.; Gonze, X. Temperature dependence of electronic eigenenergies in the adiabatic harmonic approximation. *Physical Review B* **2014**, *90*, 214304.
- (29) Allen, P. B. Theory of thermal expansion: Quasi-harmonic approximation and corrections from quasi-particle renormalization. *Modern Physics Letters B* **2020**, *34*, 2050025.
- (30) Nath, P.; Plata, J. J.; Usanmaz, D.; Al Orabi, R. A. R.; Fornari, M.; Nardelli, M. B.; Toher, C.; Curtarolo, S. High-throughput prediction of finite-temperature properties using the quasi-harmonic approximation. *Computational Materials Science* **2016**, *125*, 82–91.
- (31) Asker, C.; Belonoshko, A. B.; Mikhaylushkin, A. S.; Abrikosov, I. A. First-principles solution to the problem of Mo lattice stability. *Physical Review B* **2008**, *77*, 220102.
- (32) Asker, C. Effects of disorder in metallic systems from First-Principles calculations. Ph.D. thesis, Linköping University Electronic Press, 2010.
- (33) Yang, F.; Muñoz, J.; Hellman, O.; Mauger, L.; Lucas, M.; Tracy, S.; Stone, M.; Abernathy, D.; Xiao, Y.; Fultz, B. Thermally Driven Electronic Topological Transition in FeTi. *Physical Review Letters* **2016**, *117*, 076402.
- (34) Allen, P. B.; Heine, V. Theory of the temperature dependence of electronic band structures. *Journal of Physics C: Solid State Physics* **1976**, *9*, 2305.

- (35) Allen, P. B. Solids with thermal or static disorder. I. One-electron properties. *Physical Review B* **1978**, *18*, 5217.
- (36) Allen, P. B.; Hui, J. C. K. Thermodynamics of solids: Corrections from electron-phonon interactions. *Zeitschrift für Physik B Condensed Matter* **1980**, *37*, 33–38.
- (37) Allen, P. B.; Cardona, M. Temperature dependence of the direct gap of Si and Ge. *Physical Review B* **1983**, *27*, 4760.
- (38) Allen, P. B. Zero-point and isotope shifts: relation to thermal shifts. *Philosophical Magazine B* **1994**, *70*, 527–534.
- (39) Fan, H. Y. Temperature dependence of the energy gap in semiconductors. *Physical Review* **1951**, *82*, 900.
- (40) Migdal, A. B. Interaction between electrons and lattice vibrations in a normal metal. *Soviet Physics–JETP* **1958**, *7*, 996–1001.
- (41) Antončík, E. On the theory of temperature shift of the absorption curve in non-polar crystals. *Czechoslovak Journal of Physics* **1955**, *5*, 449–461.
- (42) Marini, A. Ab initio finite-temperature excitons. *Physical Review Letters* **2008**, *101*, 106405.
- (43) Giustino, F.; Louie, S. G.; Cohen, M. L. Electron-phonon renormalization of the direct band gap of diamond. *Physical Review Letters* **2010**, *105*, 265501.
- (44) Antonius, G.; Poncé, S.; Boulanger, P.; Côté, M.; Gonze, X. Many-body effects on the zero-point renormalization of the band structure. *Physical Review Letters* **2014**, *112*, 215501.
- (45) Poncé, S.; Antonius, G.; Boulanger, P.; Cannuccia, E.; Marini, A.; Côté, M.; Gonze, X. Verification of first-principles codes: Comparison of total energies, phonon frequencies,

- electron–phonon coupling and zero-point motion correction to the gap between ABINIT and QE/Yambo. *Computational Materials Science* **2014**, *83*, 341–348.
- (46) Poncé, S.; Gillet, Y.; Laflamme Janssen, J.; Marini, A.; Verstraete, M.; Gonze, X. Temperature dependence of the electronic structure of semiconductors and insulators. *The Journal of Chemical Physics* **2015**, *143*, 102813.
- (47) Antonius, G.; Poncé, S.; Lantagne-Hurtubise, E.; Auclair, G.; Gonze, X.; Côté, M. Dynamical and anharmonic effects on the electron-phonon coupling and the zero-point renormalization of the electronic structure. *Physical Review B* **2015**, *92*, 085137.
- (48) Patrick, C. E.; Giustino, F. Unified theory of electron–phonon renormalization and phonon-assisted optical absorption. *Journal of Physics: Condensed Matter* **2014**, *26*, 365503.
- (49) Zacharias, M.; Giustino, F. One-shot calculation of temperature-dependent optical spectra and phonon-induced band-gap renormalization. *Physical Review B* **2016**, *94*, 075125.
- (50) Friedrich, M.; Riefer, A.; Sanna, S.; Schmidt, W.; Schindlmayr, A. Phonon dispersion and zero-point renormalization of LiNbO₃ from density-functional perturbation theory. *Journal of Physics: Condensed Matter* **2015**, *27*, 385402.
- (51) Nery, J. P.; Allen, P. B.; Antonius, G.; Reining, L.; Miglio, A.; Gonze, X. Quasiparticles and phonon satellites in spectral functions of semiconductors and insulators: Cumulants applied to the full first-principles theory and the Fröhlich polaron. *Phys. Rev. B* **2018**, *97*, 115145.
- (52) Tutchton, R.; Marchbanks, C.; Wu, Z. Structural impact on the eigenenergy renormalization for carbon and silicon allotropes and boron nitride polymorphs. *Physical Review B* **2018**, *97*, 205104.

- (53) Querales-Flores, J. D.; Cao, J.; Fahy, S.; Savić, I. Temperature effects on the electronic band structure of PbTe from first principles. *Physical Review Materials* **2019**, *3*, 055405.
- (54) Miglio, A.; Brousseau-Couture, V.; Godbout, E.; Antonius, G.; Chan, Y.-H.; Louie, S. G.; Côté, M.; Giantomassi, M.; Gonze, X. Predominance of non-adiabatic effects in zero-point renormalization of the electronic band gap. *Npj Computational Materials* **2020**, *6*, 1–8.
- (55) Gonze, X.; Amadon, B.; Anglade, P.-M.; Beuken, J.-M.; Bottin, F.; Boulanger, P.; Bruneval, F.; Caliste, D.; Caracas, R.; Côté, M. et al. ABINIT: First-principles approach to material and nanosystem properties. *Computer Physics Communications* **2009**, *180*, 2582–2615.
- (56) Gonze, X.; Jollet, F.; Araujo, F. A.; Adams, D.; Amadon, B.; Applencourt, T.; Audouze, C.; Beuken, J.-M.; Bieder, J.; Bokhanchuk, A. et al. Recent developments in the ABINIT software package. *Computer Physics Communications* **2016**, *205*, 106–131.
- (57) ABINIT, Tutorial TDepES, Temperature-DEPendency of the Electronic Structure., <https://docs.abinit.org/tutorial/tdepes/>, Accessed: 2020-03-15.
- (58) Grimme, S. Semiempirical GGA-type density functional constructed with a long-range dispersion correction. *Journal of Computational Chemistry* **2006**, *27*, 1787–1799.
- (59) Grimme, S.; Ehrlich, S.; Goerigk, L. Effect of the damping function in dispersion corrected density functional theory. *Journal of Computational Chemistry* **2011**, *32*, 1456–1465.
- (60) Van Troeye, B.; Torrent, M.; Gonze, X. Interatomic force constants including the DFT-D dispersion contribution. *Physical Review B* **2016**, *93*, 144304.
- (61) Raffy, C.; Furthmüller, J.; Bechstedt, F. Properties of hexagonal polytypes of group-IV elements from first-principles calculations. *Physical Review B* **2002**, *66*, 075201.

- (62) Fan, Q.; Chai, C.; Wei, Q.; Wong, K.; Liu, Y.; Yang, Y. Theoretical investigations of group IV alloys in the Lonsdaleite phase. *Journal of Materials Science* **2018**, *53*, 2785–2801.
- (63) Stöhr, M.; Van Voorhis, T.; Tkatchenko, A. Theory and practice of modeling van der Waals interactions in electronic-structure calculations. *Chem. Soc. Rev.* **2019**, *48*, 4118–4154.
- (64) Xu, W.-W.; Xia, F.; Chen, L.; Wu, M.; Gang, T.; Huang, Y. High-temperature mechanical and thermodynamic properties of silicon carbide polytypes. *Journal of Alloys and Compounds* **2018**, *768*, 722–732.
- (65) Moruzzi, V. L.; Janak, J. F.; Schwarz, K. Calculated thermal properties of metals. *Physical Review B* **1988**, *37*, 790.
- (66) Miedema, P. S.; Beye, M.; Könnecke, R.; Schiwietz, G.; Föhlisch, A. Thermal evolution of the band edges of 6H-SiC: X-ray methods compared to the optical band gap. *Journal of Electron Spectroscopy and Related Phenomena* **2014**, *197*, 37–42.
- (67) Togo, A.; Tanaka, I. First principles phonon calculations in materials science. *Scripta Materialia* **2015**, *108*, 1–5.
- (68) Nath, P.; Plata, J. J.; Usanmaz, D.; Al Orabi, R. A. R.; Fornari, M.; Nardelli, M. B.; Toher, C.; Curtarolo, S. High-throughput prediction of finite-temperature properties using the quasi-harmonic approximation. *Computational Materials Science* **2016**, *125*, 82–91.
- (69) Harrison, W. A. *Solid state theory*; Dover, 1980.
- (70) Zywietz, A.; Karch, K.; Bechstedt, F. Influence of polytypism on thermal properties of silicon carbide. *Physical Review B* **1996**, *54*, 1791.

Supplementary Information

In the Supplementary Information, we present: (i) Proof of linearity of the EPI correction to the total energy and (ii) Results of EPI corrections to the total energy for the GGA.fhi (PBE) and the pspnc (LDA) pseudopotentials for Si, C and SiC polytypes.

Proof that $\Delta E_{av}^{ep}(T)$ varies linearly with $1/N_q$

For brevity, we represent $\Delta\epsilon_{n\mathbf{k}}(T)$ as $\Delta\epsilon_{n\mathbf{k}}$. Given that $\Delta\epsilon_{n\mathbf{k}}$ is linear in x ($= 1/N_q$) for all n, \mathbf{k} , there are constants, $a_{n\mathbf{k}}$ and $b_{n\mathbf{k}}$ such that:

$$\Delta\epsilon_{n\mathbf{k}}(x) = a_{n\mathbf{k}}x + b_{n\mathbf{k}} \quad (\text{S1})$$

The converged eigenvalue, $\Delta\epsilon_{n\mathbf{k}}^c$, is given by:

$$\Delta\epsilon_{n\mathbf{k}}^c = \lim_{x \rightarrow 0^+} \Delta\epsilon_{n\mathbf{k}}(x) = b_{n\mathbf{k}} \quad (\text{S2})$$

Substituting Eq. (S1) in Eq. (S2), we get:

$$\Delta E_{av}^{ep}(x) = 2x \sum_{n\mathbf{k}}^{occ,IBZ} w_{\mathbf{k}} a_{n\mathbf{k}} + 2 \sum_{n\mathbf{k}}^{occ,IBZ} w_{\mathbf{k}} b_{n\mathbf{k}} \quad (\text{S3})$$

The converged value of the EPI correction to the total energy, $\Delta E_{av}^{ep,c}$, is given by:

$$\Delta E_{av}^{ep,c} = \sum_{n\mathbf{k}}^{occ,IBZ} w_{\mathbf{k}} \Delta\epsilon_{n\mathbf{k}}^c = 2 \sum_{n\mathbf{k}}^{occ,IBZ} w_{\mathbf{k}} b_{n\mathbf{k}} \quad (\text{S4})$$

Therefore,

$$\Delta E_{av}^{ep,c} = \lim_{x \rightarrow 0^+} E_{av}^{ep}(x) \quad (\text{S5})$$

It follows from Eq. (S3) and Eq. (S5) that $\Delta E_{av}^{ep}(T)$ varies linearly with $1/N_q$ and the converged value can be obtained by linear extrapolation.

Si and C polymorphs

Figure S1 shows the convergence behavior of the EPI correction to the total energy with q-point grid density, using the GGA.fhi pseudopotential.

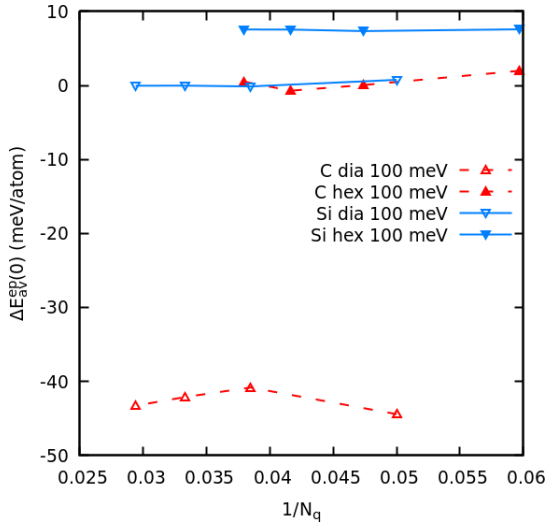


Figure S1: Convergence of electron-phonon interaction correction to the total energy with q-point grid density for smearing parameter value of 100 meV for carbon and silicon polytypes for GGA.fhi pseudopotential.

Table S1 gives the lattice parameters, band gaps and the relative energy stability with and without EPI corrections for the C and Si polymorphs. The increase in relative stability of C-dia and Si-dia is clearly seen when the EPI corrections to the total energies are included.

Figure S2 shows the convergence behavior of the EPI correction to the total energy with q-point grid density using the pspnc pseudopotential.

Table S1: The lattice parameters, band gaps and the energy differences for carbon and silicon polytypes for GGA.fhi pseudopotential

Material	a,c (Bohr)	Band gaps (Indirect/ Direct) (eV)	ΔE (DFT) (meV/f.u.)	ΔE (DFT+EPI) (meV/f.u.)
C-dia	6.73	4.21, 5.62	0	0
C-hex	4.732, 7.876	3.38, 5.0	24.9	68.7
Si-dia	10.33	0.614, 2.56	0	0
Si-hex	7.27, 12.017	0.45, 0.98	9.8	17.4

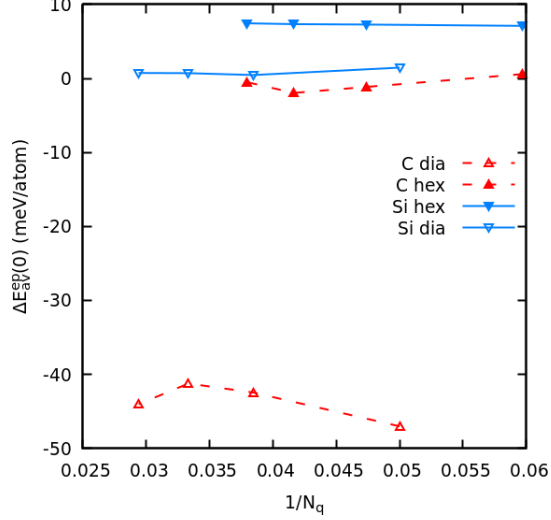


Figure S2: Convergence of electron-phonon interaction correction to the total energy with q-point grid density for smearing parameter value of 100 meV for carbon and silicon polytypes for pspnc (LDA) pseudopotential.

Table S2 gives the lattice parameters, band gaps and the relative energy stability with and without EPI corrections for the C and Si polymorphs. The increase in relative stability of C-dia and Si-dia is clearly seen when the EPI corrections to the total energies are included.

Table S2: The lattice parameters, band gaps and the energy differences for carbon and silicon polytypes for pspnc pseudopotential

Material	a,c (Bohr)	Band gaps (Indirect/ Direct) (eV)	ΔE (DFT) (meV/f.u.)	ΔE (DFT+EPI) (meV/f.u.)
C-dia	6.69	4.22, 5.63	0	0
C-hex	4.706, 7.838	3.12, 4.99	24.8	68.5
Si-dia	10.20	0.43, 2.52	0	0
Si-hex	7.180, 11.875	0.26, 0.95	8.4	15.1

The above results are similar to those for ONCV pseudopotential in the main paper.

SiC polytypes

We first present results for SiC polytypes obtained using GGA.fhi pseudopotential.

Table S3: The lattice parameters and the energy stability of SiC polytypes relative to SiC-3C for DFT, DFT-D2 and DFT-D3(BJ) conditions for GGA.fhi pseudopotential.

Polytype	a,c (Bohr)	ΔE (meV/SiC)
3C-SiC		
DFT	8.26	0
DFT-D2	8.21	0
DFT-D3(BJ)	8.20	0
4H-SiC		
DFT	5.834, 19.099	-2.11
DFT-D2	5.799, 19.014	2.54
DFT-D3(BJ)	5.788, 18.498	-1.84
2H-SiC		
DFT	5.831, 9.568	4.98
DFT-D2	5.795, 9.537	14.5
DFT-D3(BJ)	5.784, 9.491	6.02

Table S3 shows the lattice parameters and the energy stabilities relative to the SiC-3C polytype for DFT condition and also when dispersion approximations are included. We see that SiC-4H is more stable than SiC-3C for DFT conditions. When vdW-D2 approximation is included, SiC-3C is the stable structure, similar to literature results. However, when vdW-D3(BJ) approximation is used, SiC-4H is more stable. This is similar to the results for the ONCV pseudopotential reported in the main paper.

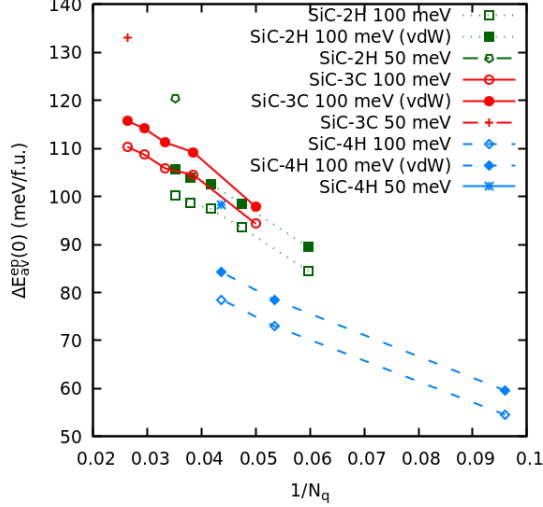


Figure S3: Convergence of EPI correction to the total energy with q-point grid density for different smearing parameters for SiC polytypes for DFT and DFT-D3(BJ) lattice parameters for GGA.fhi pseudopotential.

Figure S3 shows the convergence behaviour of the EPI correction to the total energy with q-point grid density for SiC polytypes for different smearing parameters. For 100 meV smearing parameter, the $\Delta E_{av}^{ep}(0)$ was calculated only upto $\frac{1}{N_q} \approx 0.043$ due to computational limitations. For 50 meV smearing parameter, only the results for the highest q-point grid density was calculated (due to computational limitations.)

Table S4: Relative stability (in meV/f.u.) of SiC polytypes using GGA.fhi pseudopotential in non-adiabatic condition-100meV smearing parameter. vdW represents results from DFT+D3(BJ) calculations .

Polytype→ Stability ↓	SiC-3C	SiC-4H	SiC-2H
DFT	0	-2.1	5.0
DFT + vdW	0	-1.8	6.0
DFT + EPI (100 meV)	0	-33.9/-28.1	-5.1
DFT + vdW + EPI (100 meV)	0	-33.4/-26.8	-4.1
DFT + vdW + EPI (50 meV)	0	-36.6	-6.7

Table S4 shows the final stability of SiC-polytypes obtained by combining the EPI corrections in Figure S3 with the relative stability data in Table S3. For SiC-3C and SiC-2H we consider the last value to be the converged value. However, for SiC-4H, the last calculated value ($\frac{1}{N_q} \approx 0.043$) is not the converged value as it varies by $\lesssim 6$ meV/f.u. compared to

the previous value. Therefore, for SiC-4H, we report two values in Table S4; the first is the difference between the last values for SiC-3C and SiC-4H and the second is the difference at $\frac{1}{N_q} \approx 0.043$ for SiC-4H and the nearest value for SiC-3C, $\frac{1}{N_q} \approx 0.039$. The actual stability value of for SiC-4H is likely to be between these two values.

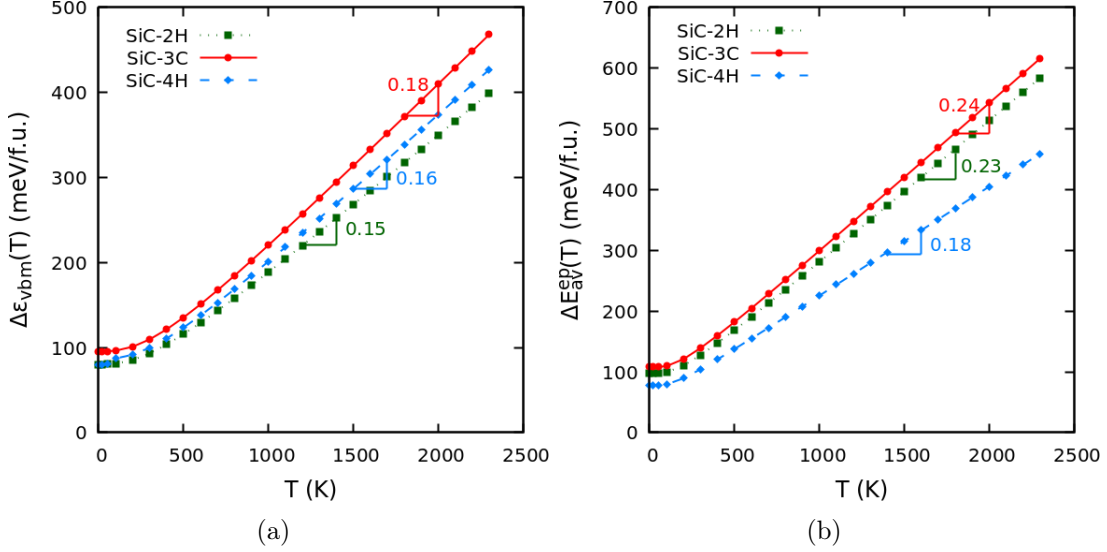


Figure S4: Finite temperature EPI corrections to (a) VBM and (b) total energy of SiC for DFT-D3(BJ) lattice parameters for GGA.fhi pseudopotential.

Figure S4 shows temperature dependence of the EPI correction to VBM and the total energy for SiC polytypes for GGA.fhi pseudopotential.

The results using GGA.fhi pseudopotential are similar to those from ONCV-PBE pseudopotential presented in the main paper.

Table S5 shows the lattice parameters and the energy stabilities relative to the SiC-3C polytype using the pspnc pseudopotential. The vdW corrections were not performed because ABINIT package does not support DFT-D2 and DFT-D3(BJ) corrections for LDA pseudopotentials.

Table S5: The lattice parameters and the energy stability (DFT) in meV/f.u. of SiC polytypes relative to SiC-3C for DFT lattice parameters for pspnc pseudopotential.

Polytype	a,c (Bohr)	ΔE (DFT) (meV/SiC)
3C-SiC	8.18	0
4H-SiC	5.782, 18.931	-3.17
2H-SiC	5.778, 9.485	4.33

Figure S5 shows the convergence behaviour of the EPI correction to the total energy with q-point grid density for SiC polytypes for different smearing parameters. For 100 meV smearing parameter, the $\Delta E_{av}^{ep}(0)$ was calculated only upto $\frac{1}{N_q} \approx 0.043$ due to computational limitations. For 50 meV smearing parameter, only the results for the highest q-point grid density was calculated (due to computational limitations.)

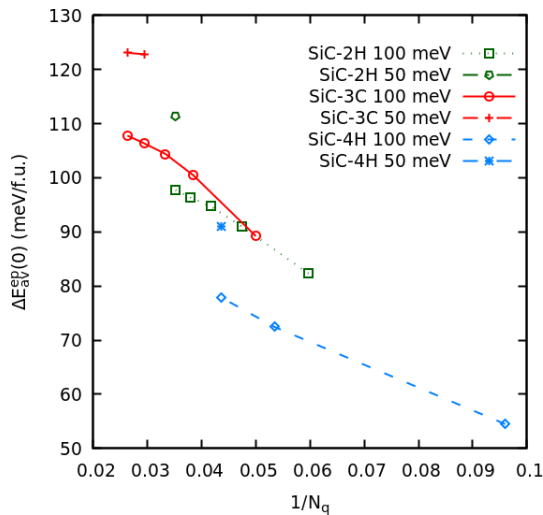


Figure S5: Convergence of electron-phonon interaction correction to the total energy with q-point grid density for different values of the smearing parameter for SiC polytypes for pspnc (LDA) pseudopotential.

Table S6: Relative stability (in meV/f.u.) of SiC polytypes using pspnc pseudopotential in non-adiabatic condition-100 meV and 50 meV smearing parameters.

Polytype→ Stability ↓	SiC- 3C	SiC-4H	SiC-2H
DFT	0	-3.2	4.3
DFT + EPI (100 meV)	0	-33.1/- 25.8	-5.7
DFT + EPI (50 meV)	0	-35.2	-7.3

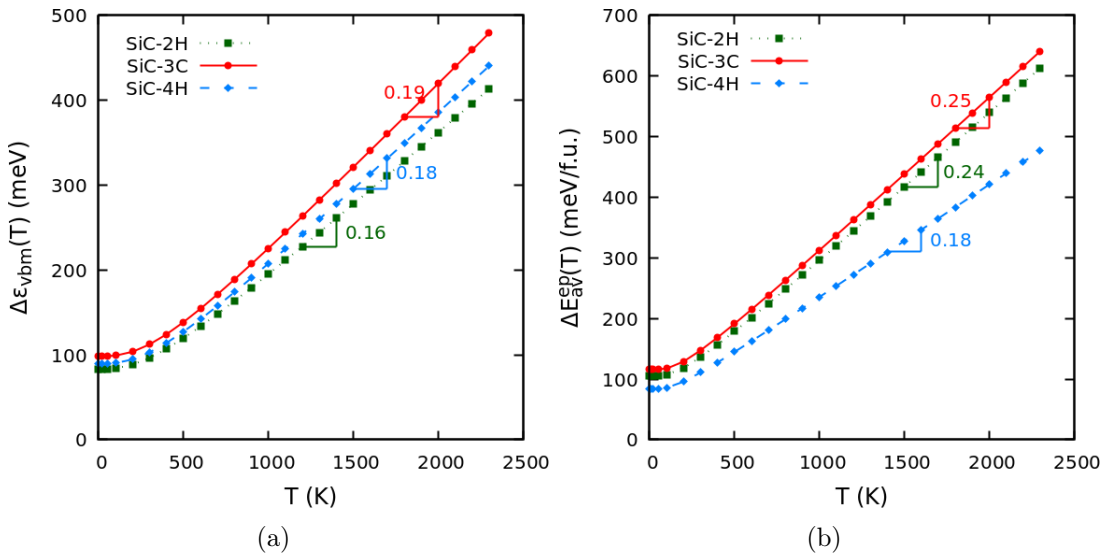


Figure S6: Finite temperature EPI corrections to (a) VBM and (b) total energy of SiC for DFT lattice parameters for LDA pseudopotential.

Table S6 shows the final stability of SiC-polytypes obtained by combining the EPI corrections in Figure S4 with the relative stability data in Table S5. For SiC-3C and SiC-2H we consider the last value to be the converged value. However, for SiC-4H, the last calculated value ($\frac{1}{N_q} \approx 0.043$) is not the converged value as it varies by $\lesssim 6$ meV/f.u. compared to the previous value. Therefore, for SiC-4H, we report two values in Table S4; the first is the difference between the last values for SiC-3C and SiC-4H and the second is the difference at $\frac{1}{N_q} \approx 0.043$ for SiC-4H and the nearest value for SiC-3C, $\frac{1}{N_q} \approx 0.039$. The actual stability value of for SiC-4H is likely to be between these two values.

Figure S6 shows temperature dependence of the EPI correction to VBM and the total energy for SiC polytypes for pspnc pseudopotential.

The results using pspnc pseudopotential are similar to those from the ONCV pseudopotential presented in the main paper.

Our results from both the GGA.fhi and the pspnc pseudopotentials are similar to those from ONCV pseudopotential. This suggests that the results are stable and independent of the choice of the pseudopotential.